CHARACTERIZATION OF THE INTERNAL PLASMA STRUCTURE OF A 5 KW HALL THRUSTER

James M. Haas[1] and Alec D. Gallimore[2]
Plasmadynamics and Electric Propulsion Laboratory
Department of Aerospace Engineering
The University of Michigan
College of Engineering
Ann Arbor, MI 48109 USA

ABSTRACT

The Plasmadynamics and Electric Propulsion Laboratory (PEPL) High-speed Axial Reciprocating Probe (HARP) system is used in conjunction with a floating emissive probe to measure plasma potential in the discharge chamber of the P5 Hall thruster. Plasma potential measurements are made at a constant voltage, 300 V, at two different discharge current conditions: 5.4 A, and 10 A. The plasma potential contours for the 5.4 A case indicate that the acceleration region begins several millimeters upstream of the exit plane, extends several centimeters downstream, and is uniform across the width of the discharge chamber. The 10 A case is similar to the 5.4 A case with the exception that the acceleration region is shifted downstream on center line. Axial electric field profiles, computed from the measured potential, show a double peak structure in the 5.4 A case, indicating a local ion deceleration. Perturbations to the discharge current are shown to correspond spatially with the location of the peak electric field indicating that thruster perturbations may result from a disturbance to the Hall current, as opposed to, or in addition to, ablation of probe material.

INTRODUCTION

The role of Hall thrusters in spacecraft propulsion is constantly evolving and expanding as new missions, covering the full spectrum of spacecraft size and power, continue to be developed. A large number of such missions can significantly benefit from the unique performance characteristics of Hall thrusters. These range from sub-kW thrusters for micro-satellites, to 1.5 kW thrusters for station-keeping, to high power thrusters for orbit raising/transfer applications.[1-4]

While a number of Hall thrusters have been, or are in the process of being, flight qualified[5-6] many of the basic physical processes inside the Hall thruster are still not fully understood. In order to improve the performance of the next generation of thrusters, as well as to address spacecraft interaction issues, the ionization and acceleration mechanisms inside the discharge chamber of the Hall thruster must be better understood. Toward this end, the Plasmadynamics and Electric Propulsion Laboratory (PEPL) at the University of Michigan has constructed a laboratory model Hall thruster, designated the P5, designed specifically to facilitate measurements in the discharge chamber.[7] As part of the same program, PEPL has constructed and successfully demonstrated a High-speed Axial Reciprocating Probe[8] (HARP) to allow electrostatic probe measurements without significantly perturbing thruster operation. This is accomplished by inserting and removing probes on time scales such that the probe does not heat to the point where probe material is ablated.

In addition to providing direct insight on the ionization and acceleration mechanisms, data on the internal plasma structure will play a valuable role in validating existing and future numerical models.[9-10] The increasing time and expense associated with developing new thrusters makes it imperative that accurate and reliable predictive models are developed.

OBJECTIVE

The objective of this research is to measure the plasma potential inside the discharge chamber of a Hall thruster while avoiding significant perturbation to thruster operation. The resulting data are used to determine the magnitude and spatial structure of the acceleration region as well as to better understand the role of the Hall current in thruster operation.

---

[1] Ph.D. Candidate, Aerospace Engineering.
[2] Associate Professor, Aerospace Engineering and Applied Physics.

Copyright © 1999 James M. Haas.
Published by the Japan Society for Aeronautical and Space Sciences with permission.

EXPERIMENTAL SET-UP

Vacuum Chamber

All experiments are conducted in the University of Michigan's 6 m diameter by 9 m long Large Vacuum Test Facility (LVTF). The pumping system consists of four CVI model TM-1200 Re-Entrant Cryopumps providing a measured Xenon pumping speed of 140,000 l/s. The ultimate base pressure of the facility is $2x10^{-7}$ Torr. The operating pressures for this experiment are $5.5x10^{-6}$ Torr and $9.6x10^{-6}$ Torr when corrected for Xenon and corresponded to discharge currents of 5.4 A and 10.0 A, respectively. Details of the facility have been presented in a previous work.[7]

Thruster

The thruster used is the University of Michigan/Air Force Research Laboratory P5 5 kW laboratory model Hall thruster. This thruster was developed specifically for diagnostic access to the discharge chamber. Compared to smaller thrusters, the P5 provides a larger discharge chamber for better spatial resolution for electrostatic probes as well as a lower power density to reduce heat flux to the probe. Thrust, specific impulse, and efficiency have been characterized thoroughly and have been reported, along with plasma parameter profiles in the plume, in a previous work.[7] The P5 incorporates a Lanthanum Hexaboride (LaB6) cathode provided by the Moscow Aviation Institute (MAI).

Emissive Probe

Plasma potential measurements are made using a floating emissive probe. Figure 1 shows a schematic of the probe construction.

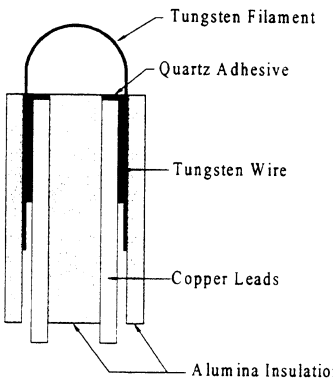

Figure 1. Shown is a schematic of the emissive probe showing its individual parts and construction. When heated to the point where electrons are emitted, the probe floats at the local plasma potential.

The emitting portion of the probe is a filament made from 0.127 mm diameter tungsten wire. The ends of this filament are inserted approximately 76 mm down a 152 mm length of double bore alumina tubing along with 30 AWG copper wire leads. Once the tungsten filament and copper leads are in place additional, shorter lengths of tungsten wire are inserted into the alumina tubing to provide a tight fit and guarantee good contact between the tungsten and copper wires.

The theory of the floating emissive probe is well established and relatively straight forward to implement.[11] The circuit consists of the emissive probe, a floating power supply capable of supplying enough current to heat the filament (4 A – 7 A), and a voltage meter. Figure 2 shows a schematic of the probe circuit.

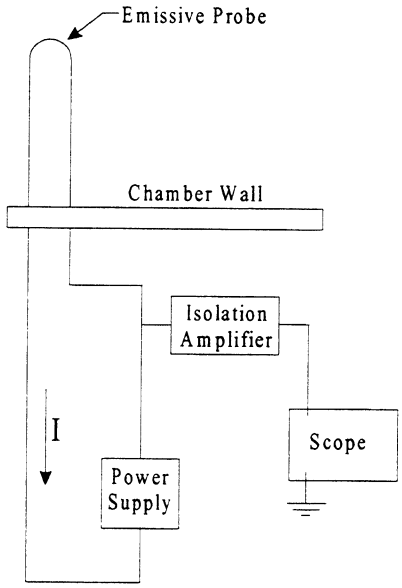

Figure 2. The floating emissive probe circuit consists of a current source to heat the filament and an oscilloscope for measuring the resulting floating/plasma potential.

The power supply provides current to heat the filament to the point where it is thermionically emitting sufficient electrons to neutralize the sheath. At this point, the probe will float at the local plasma potential. This heater current varied between tests due to slight variations in individual probe designs, ranging between 4.5 – 6.0 A. The probe potential is divided and sent through an isolation amplifier capable of floating its input as high as 2500 V. The output is a ±10 V signal referenced to ground. Because the heater current remains on during the duration of the measurement, a voltage drop exists across the tungsten filament. This value remains below 5 V for each data sweep, thus the potential measurements contain an estimated uncertainty of approximately ±2.5 V. An analysis by Hargus[14], taking into account the apparent plasma potential to probe filament current, indicates an uncertainty of approximately –3/+6 V.

Positioning System

The emissive probe is positioned inside the Hall thruster discharge chamber using the PEPL HARP system. The HARP system allows the probe to be inserted into, and removed from, the thruster on a time scale under 100 ms. This allows measurements to be made with very little perturbation to thruster operation. The extent of thruster perturbation is determined by monitoring the discharge current during probe movement. Use of the emissive probe causes a slight perturbation in the discharge current but this remains less than 15% of the nominal discharge current value during all measurements. Potential data are taken during both insertion and removal of the probe and for the majority of the axial sweeps, the two traces are the same. In some cases, the two traces differed slightly and it is assumed that the probe material is beginning to ablate by the time the probe is removed. Thus the inward sweep is considered to be the more accurate of the two. In order to be consistent, all data presented in this paper, except where noted, are from the inward sweep.

Figure 3 shows the area inside the discharge chamber where plasma potential is measured.

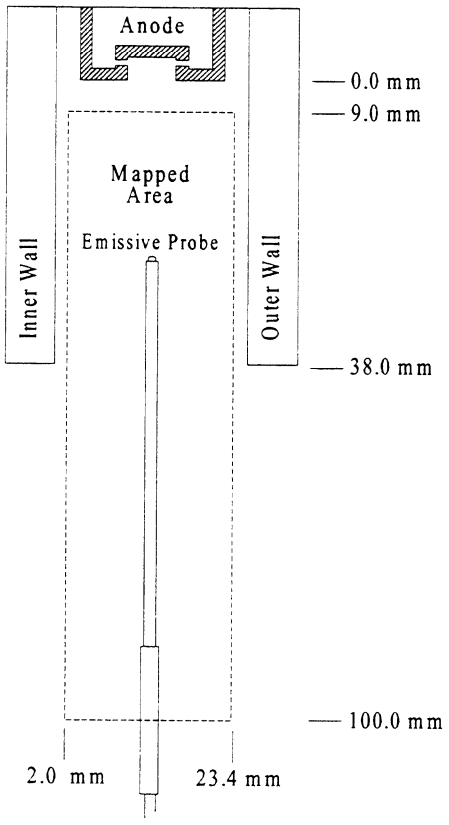

Figure 3. The area mapped begins approximately 8 mm from the anode face, extends 10 cm downstream of the exit plane, and comes to within 2 mm of the inner and outer walls of the discharge chamber.

Radial movement is accomplished by mounting the thruster on a linear table. Between axial sweeps with the HARP system, the thruster is moved radially such that a 2-D cross section of the discharge chamber is covered. Note that the axial position throughout this paper corresponds to the tip of the filament.

RESULTS AND DISCUSSION

Plasma potential measurements with respect to ground are made at a constant voltage, 300 V, at discharge current settings of 5.4 A and 10 A. Figure 4 shows three representative potential profiles at 300 V, 5.4 A: on center line and along the inner and outer walls. For this case, the cathode potential with respect to ground is –21 V, therefore the anode is sitting at a potential of 279 V with respect to ground.

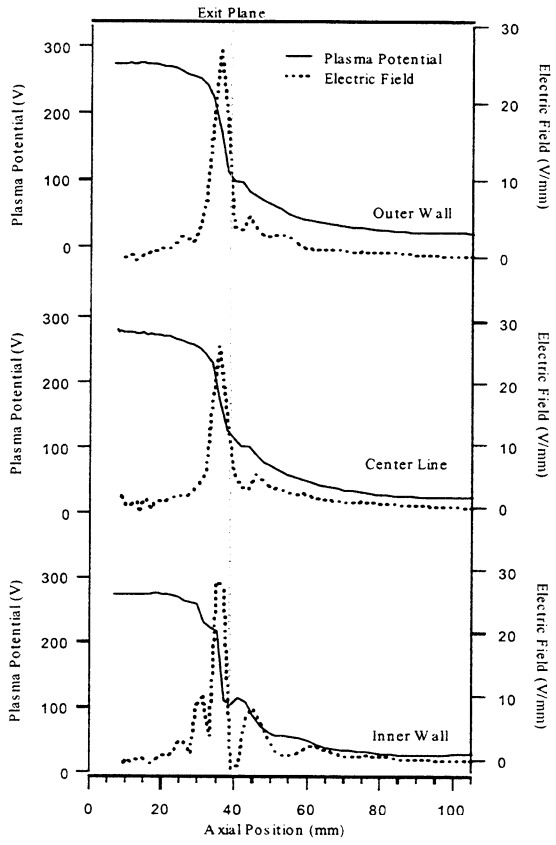

Figure 4. Shown are the plasma potential and axial electric field profiles at three representative radial locations for the 300 V, 5.4 A case. The anode face corresponds to a position of 0 mm and the exit plane, as marked, is at a position of 38 mm.

Plasma potential profiles for the 5.4 A case show that the potential remains nearly constant over the first 75% of the channel. As expected, a sharp drop occurs between 30 mm and 40 mm indicating the

location of the main acceleration region. The axial electric field profiles show clearly the location of maximum acceleration at 35.5 mm, 2.5 mm upstream of the exit plane. The data indicate that the acceleration region extends 2 – 3 cm downstream of the exit plane which agrees quite well with independent LIF[12] data taken on the same thruster at the same conditions. The data also agree with potential measurements from other Hall thrusters.[13] Note that the profile remains uniform across the width of the discharge chamber which is also consistent with LIF data.[12]

One feature of the potential data that bears further scrutiny is the "bump" that occurs approximately 5 mm downstream of the exit plane, most prominently seen on the inner wall profile. This will be discussed further below.

Potential data are also taken at a higher power level to study the evolution of the potential structure. Figure 5 shows plasma potential profiles at 300 V, 10 A at the same three radial positions as in Figure 4. Cathode and anode potentials with respect to ground are –23 V and 277 V, respectively.

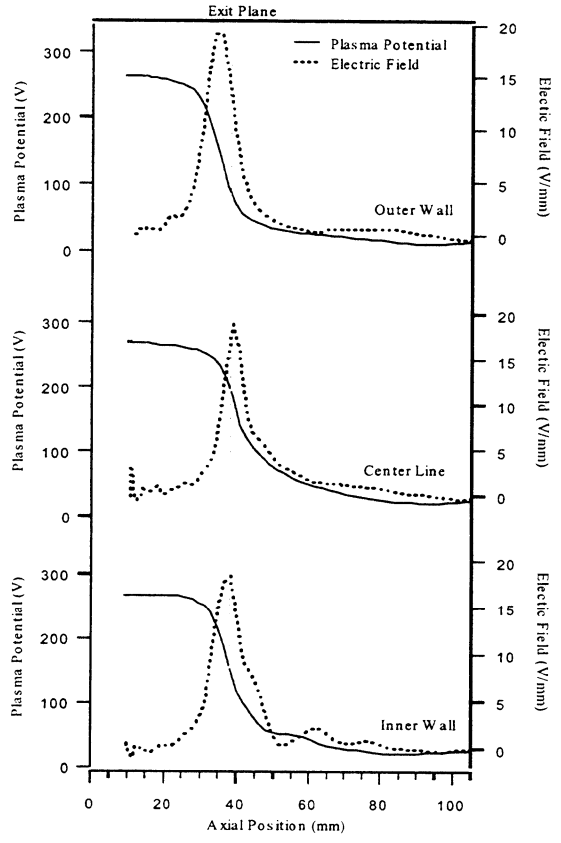

Figure 5. Plasma potential and axial electric field profiles at three representative radial locations for the 300 V, 10 A case. The anode face corresponds to a position of 0 mm and the exit plane, as marked, is at a position of 38 mm.

These data are very similar to the 5.4 A case. The potential remains approximately constant, at anode potential, over the first 75% of the discharge channel. The acceleration region begins near the exit plane and extends several centimeters downstream. Notice, however, that the axial electric field at 10 A is nearly 25% percent lower, indicating a longer acceleration region. Baranov[16] shows that the length of the acceleration layer depends on both the magnetic field profile and electron temperature. For the two cases considered here, the magnetic field profile (both magnitude and shape) is kept constant and only the mass flow rate is adjusted. This increase in mass flow rate effectively increases the ionization collision frequency, lowering the energy of the electrons since the ionization process is a loss mechanism. The result is a lower temperature gradient, therefore lower electric field. The reduction of temperature gradients with increasing discharge current is predicted by the one-dimensional code of Ahedo[18] and is consistent with the data in figure 5.

The potential and electric field profiles at 10 A are also not uniform across the width of the discharge chamber. Looking at the axial electric field profiles, the peak along the outer wall occurs 2 mm – 3 mm upstream of the exit plane as in the 5.4 A case. Along the inner wall, the peak is shifted forward but still occurs upstream of the exit plane. The most significant difference between the two cases is seen in the center line data where the peak electric field is shifted to a position downstream of the exit plane. As with the electric field magnitude, since the magnetic field is unchanged, this implies a shift in the electron temperature gradient. This may occur due to the higher density of ions on centerline retarding the flow of high-energy electrons toward the anode. It follows that this effect would be less pronounced along the walls because of increased ion losses resulting from a longer acceleration region[17].

One prominent feature that is virtually nonexistent at 10 A is the "bump" in the potential profile seen at 5.4 A. This "bump" is most prominent along the inner wall where the potential exhibits a local increase in the acceleration region. The magnitude of this perturbation decreases from the inner wall, where the radial magnetic field is strongest, to the outer wall, where the radial magnetic field is lower. It is believed that this perturbation is the result of turbulence in the plasma flow as it expands out of the channel. However, a satisfactory explanation for this effect is not available at this time. It is worth noting that this feature has been observed, to a lesser extent, in other laboratory Hall thrusters as well[14].

Figures 6 and 7 are the complete set of plasma potential contours. Although figures 4 and 5 show only three representative profiles within the radial confines of the discharge channel, a total of seven

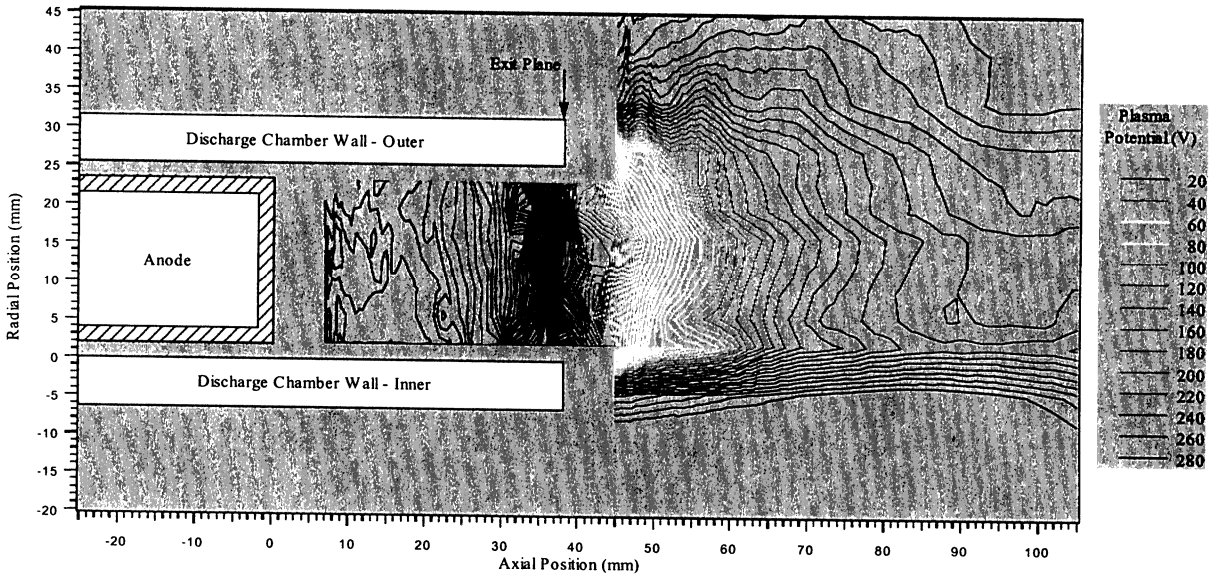

Figure 4. Shown are the plasma potential contours at a thruster operating condition of 300 V, 5.4 A. The maximum potential is 280 V with respect to ground and occurs at the anode, which is at a potential of 280 V. The potential drops sharply several millimeters upstream of the exit plane (38 mm) and continues to drop out to an axial position of 100 mm. This axial profile is uniform across the width of the discharge chamber.

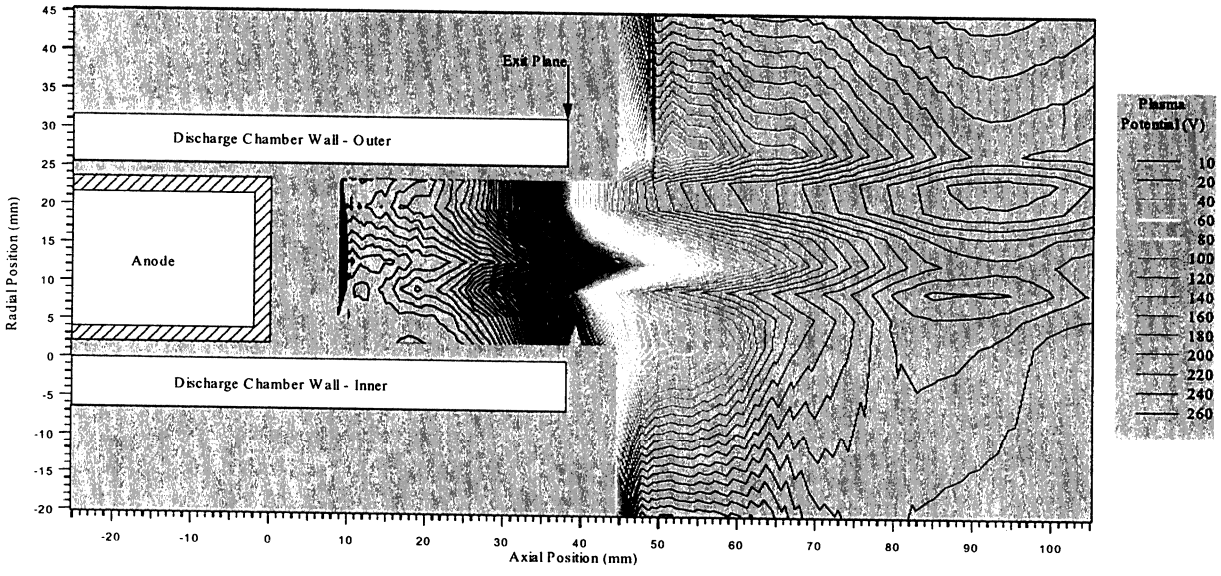

Figure 5. Shown are the plasma potential contours at a thruster operating condition of 300 V, 10 A. The maximum potential is 277 V with respect to ground and occurs at the anode, which is at a potential of 278 V. The potential drops sharply several millimeters upstream of the exit plane (38 mm) near the inner and outer walls but has a sharp drop downstream of the exit plane at the center line. Note that his case lacks the radial uniformity of the 5.4 A case.

axial sweeps are performed to improve the spatial resolution of the potential map. In addition, axial sweeps are performed at radial positions beyond the inner and outer walls to investigate ion acceleration further outside the channel. All of these sweeps are combined to generate a two-dimensional contour of the plasma potential. Figure 6 shows the plasma potential contours for the 300 V, 5.4 A case. It is not as obvious from Figure 6 that a local plateau occurs just downstream of the exit plane but the radial uniformity is clear. The contour lines of Figure 6 also show that there is a significant radial ion acceleration which has been observed by several independent diagnostics including Faraday probes[7], mass spectroscopy[15], and LIF[12].

Figure 7 shows the plasma potential contours for the 300 V, 10 A case. As mentioned previously, one way in which the plasma potentials of the 10 A case differ from those of the 5.4 A case is that the peak electric field on center line at 10 A is shifted downstream of the exit plane. This is readily apparent in Figure 7 where a potential "jet" occurs in the center of the chamber. Additional data at 10 A and 8 A, not include in this paper, show this structure to be repeatable and evolving, becoming more pronounced as the discharge current is increased. This structure results in significant divergence of the ions as they are accelerated out of the thruster.

The HARP system used in this experiment was initially tested using a triple Langmuir probe at a thruster condition of 300 V and 5.4 A.[8] At this power level, the presence of the probe appeared to not perturb thruster operation, as evidenced by the extent of discharge current perturbations during axial sweeps inside the thruster discharge chamber. Because of these results, the discharge current was not monitored during emissive probe measurements at 5.4 A. However, at 10 A, the discharge current was monitored for each axial probe sweep and a 5 – 15% variation in magnitude was observed. While zero perturbation would have been preferred, the current perturbations, when combined with the plasma potential profiles, yielded some unexpected insights. Figure 8 shows three representative traces of the discharge current and the computed axial electric field along the inner wall, outer wall, and on center line. Only three data sets are shown here, however, each axial sweep across the discharge chamber showed the same results.

From Figure 8, perturbations to the discharge current are seen to correspond very well to the spatial location of the peak axial electric field. Power deposition to the probe is proportional to the third power of the drift velocity, while the ExB drift velocity is proportional to the magnitude of the electric field. Therefore, it is expected that the probe would experience the greatest heat load where the electric field has its largest magnitude. It follows immediately that this would be the point of greatest probe material ablation and hence discharge current perturbation. However, if this were the only mechanism disturbing thruster operation, once the probe was inserted into the discharge chamber, a portion of the probe would always see this heat load, and probe material would continue to ablate. In this case, the discharge current would remain artificially high while the probe was present inside the discharge chamber. This would also be the case if the probe were simply acting as a physical barrier, impeding the motion of the electrons as they drifted azimuthally inside the thruster.

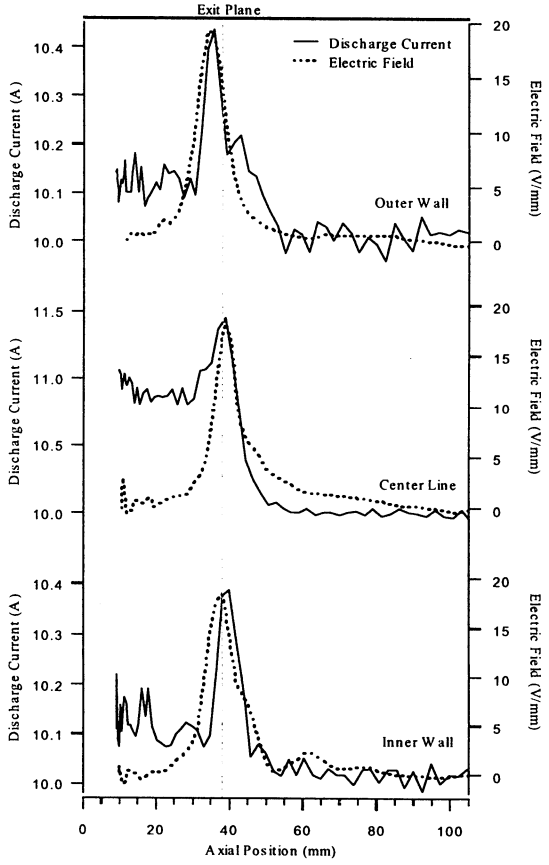

Figure 8. Perturbations in the discharge current as a function of probe position are compared to the axial electric field profiles.

Figure 9 shows a representative profile of the discharge current including both the insertion and removal of the probe. Recall that the probe assembly is 152 mm long with the emitting tungsten filament loop extending approximately 1 mm outside the alumina insulator. The axial position in Figure 9 (as in all figures in this paper) corresponds to the tip of the filament. Therefore, the greatest perturbation of the discharge current occurs when the tungsten filament is coincident with the peak axial electric

field. This implies one of two things; Either the presence of a conductor disturbs the drift current or the emitted electrons are somehow coupling with the drifting electrons, resulting in an increased discharge current. Previous experiments with the triple probe did not result in perturbations to the discharge current. However, triple probe data exists only for the 5.4 A case and discharge current was not monitored at 5.4 A with the emissive probe. Regardless, it is clear that the Hall current plays an important role in thruster operation and thruster/probe interactions and must be taken into consideration during any future internal measurements.

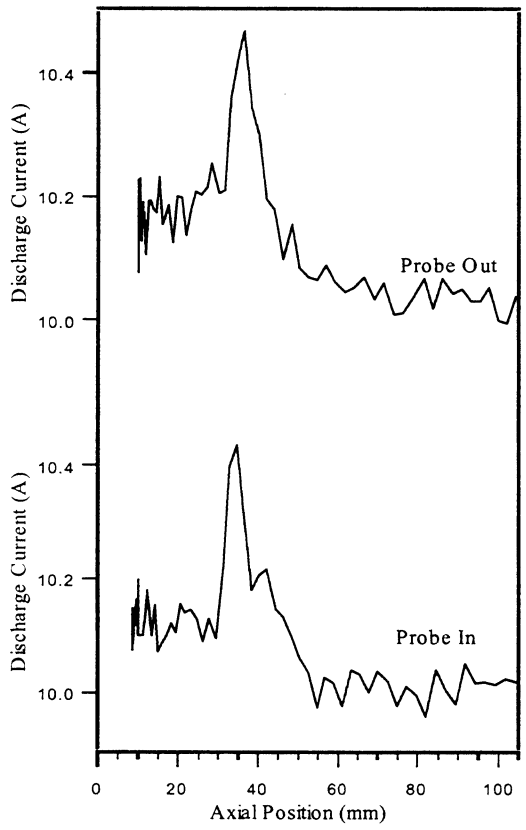

Figure 9. Discharge current as a function of probe position inside the discharge chamber.

FUTURE WORK

Investigations into the acceleration mechanisms of the Hall thruster will continue. Additional emissive probe measurements, with the filament in an emitting and non-emitting state, are planned to address issues of Hall current/electrostatic probe interactions. Single Langmuir probe measurements are planned for measurement of electron temperature and ion number density profiles. This will also provide data for comparison to triple probe results. Miniature Faraday probe measurements are also planned to determine ion flux to the walls of the discharge chamber and to map the Hall current zone.

ACKOWLEDGEMENTS

The research contained herein was sponsored by the Air Force Office of Scientific Research under Dr. Mitat Birkan; This support is gratefully acknowledged. The authors would like to thank Dr. Sergei Khartov of the Moscow Aviation Institute (MAI) for providing the cathode used in these tests. They would also like to thank their fellow researchers at PEPL for assistance during experimental set-up and operation. Mr. James Haas is supported by the United States Air Force Palace Knight Program.

REFERENCES

1 Arkhipov, B., et al., "Extending the Range of SPT Operation: Development Status of 300 and 4500 W Thrusters," AIAA 96-2708, 32nd Joint Propulsion Conference, July 1996.

2 Gallimore, A.D., et al., "Plume Characterization of the SPT-100," AIAA 96-3298, 32nd Joint Propulsion Conference, July 1996.

3 Manzella, D.H., et al., "Performance Evaluation of the SPT-140," IEPC 97-059, 25th International Electric Propulsion Conference, August 1997.

4 Tverdokhlebov, S.O., and Garkusha, V.I., "High-Voltage Mode of a TAL Thruster Operation," IEPC 97-023, 25th International Electric Propulsion Conference, August 1997.

5 Sankovic, J.M., et al., "RHETT2/EPDM Development Testing," IEPC 97-102, 25th International Electric Propulsion Conference, August 1997.

6 Garner, C.E., et al., "A 5,730-Hr Cyclic Endurance Test of the SPT-100," AIAA 95-2667, 31st Joint Propulsion Conference, July 1995.

7 Haas, J.M., et al., "Performance Characteristics of a 5 kW Laboratory Hall Thruster," AIAA 97-3503, 34th Joint Propulsion Conference, July 1998.

8 Haas, J.M., et al., "Hall Thruster Discharge Chamber Plasma Characterization Using a High-Speed Axial Reciprocating Electrostatic Probe," AIAA 99-2426, 35th Joint Propulsion Conference, June 1999.

9 Qarnain, S., and Hastings, D., "Complete Computational Model of a Hall Thruster from the Acceleration Chamber Through the Plume," IEPC 97-133, 25th International Electric Propulsion Conference, August 1997.

10 Fife, J.M., "Two-Dimensional Hybrid Particle-in-cell Modeling of Hall Thrusters." MIT department of Aeronautics and Astronautics, S.M. Thesis, Cambridge, MA, 1995.

11 Kemp, Robert F., and Sellen, J.M. Jr., "Plasma Potential Measurements by Electron Emissive Probes," *Review of Scientific Instruments,* 37(4), April 1966.
12 Williams, G.J., et al., "Laser Induced Fluorescence Measurement of Ion Velocities in the Plume of a Hall Effect Thruster," AIAA 99-2424, 35th Joint Propulsion Conference, June 1999.
13 Hargus, W.A., et. al., "A Study of a Low Power Hall Thruster Transient Behavior," IEPC 97-058, 25th International Electric Propulsion Conference, September 1997.
14 Hargus, W.A. Jr., and Cappelli, M.A., "Interior and Exterior Laser-Induced Fluorescence and Plasma Potential Measurements on a Laboratory Hall Thruster," AIAA 99-2721, 35th Joint Propulsion Conference, June 1999.
15 Gulczinski, F.S., et al., "Near-Field Ion Energy and species Measurements of a 5 kW Laboratory Hall Thruster," AIAA 99-2430, 35th Joint Propulsion Conference, June 1999.
16 Baranov, V.I., et. al., "Energy Balance and role of Walls in ACDE," IEPC 97-060, 25th International Electric Propulsion Conference, September 1997.
17 Raitses, Y., et al., "Probe Measurements of Plasma Properties Inside an Experimental Hall Thruster," AIAA 98-3640, 34th Joint Propulsion Conference, July, 1998.
18 Ahedo, E., and Martinez-Sanchez, M., "One-Dimensional Plasma Structure in Hall Thrusters," AIAA 98-8788, 34th Joint Propulsion Conference, July, 1998.